1968MNRAS.140..345F

Mon. Not. R. astr. Soc. (1968) **140**, 345–367.

THE KINEMATICS OF PLANETARY NEBULAE IN THE MAGELLANIC CLOUDS

M. W. Feast

(Communicated by the Radcliffe Observer)

(Received 1968 February 7)

Summary

Radial velocities have been determined for 25 planetary nebulae in the LMC and 11 in the SMC. Many of the observations were made at 49 Å/mm at Hγ. The planetary nebulae are the first old subsystem in the Magellanic Clouds to be studied kinematically in any detail. In addition Table I contains three objects not now considered to be planetaries including Henize SMC N55 which is an interesting [Fe II] emission line object.

In the LMC the overall rotational pattern of the planetaries agrees with that found previously for very young objects. This shows that the old and young objects belong to one (complex) system rather than being essentially independent as has sometimes been suggested; and that the displacement of the centre of rotation 1 kpc north of the optical bar is a fundamental property of LMC dynamics rather than a peculiarity restricted to the youngest objects. The planetary nebulae show a poor detailed correlation with the velocities and densities of the interstellar H I, consistent with their being old objects. A velocity dispersion of 22 ± 3 (s.e.) km s^{-1} is found, twice that of young objects. This is taken to indicate a collapse of the LMC to a plane at some time in the past (as in the Galaxy). Some indication is found that the velocity dispersion may be a function of magnitude.

In the SMC there is also poor detailed correlation between the planetary velocities and the velocities and densities of the interstellar gas. However, the marked division of the planetaries into two compact velocity groups indicates the existence of two distinct groups of objects in the same line of sight, as is also indicated by the double peaks of the 21 cm profiles. The planetaries, being old, cannot belong to the expanding shells proposed by Hindman to account for the 21 cm data. It is suggested, rather, that objects of a wide range of ages follow non-circular orbits in a barred system, the bar being seen end on with gas and stars flowing out at both ends.

As in the Galaxy the Magellanic Cloud planetaries cover a wide range of excitation classes. The frequency distribution of these classes is different in the SMC from the LMC whilst the region of the Galaxy so far surveyed is probably closer to the LMC in this respect. In the LMC high excitation objects seem to be more frequent amongst the fainter planetaries.

1. *Introduction.* During the past fifteen years radial velocity observations at optical and radio frequencies have considerably improved our understanding of the kinematics of the two Magellanic Clouds. The most recent detailed discussions of the radio work are by McGee & Milton (1966a) and Hindman (1967) and of the optical work by Feast, Thackeray & Wesselink (1961) and Feast (1964a). However, these observations refer almost entirely to the very young component in the Clouds (supergiant stars, diffuse nebulae and interstellar gas). Whilst it remains very desirable to extend the observations on these young objects, a complete understanding of the dynamics and evolution of these galaxies will only be possible

© Royal Astronomical Society • Provided by the NASA Astrophysics Data System

Downloaded from https://academic.oup.com/mnras/article/140/3/345/2602684 by guest on 20 August 2022

1968MNRAS.140..345F

when radial velocity data are available for objects covering the whole range of ages present in the Clouds. Of the older objects so far identified in the Clouds the planetary nebulae form an especially interesting group. The planetaries in the Galaxy are found to have a wide range of ages covering the period of the initial collapse of the Galaxy to a plane, with the majority constituting an old disc population (the evidence is summarized by Feast (1967)). Unless the planetary population in the Clouds is quite different from that in the Galaxy we may expect these objects to yield information on the kinematics of subsystems in the clouds very much older than those previously studied.

The discovery of planetary nebulae in the Magellanic Clouds has primarily been carried out by objective prism observations (by Lindsay, Westerlund and their collaborators) or by filter photography (Koelbloed). The various surveys are summarized by Westerlund (1967). Undoubtedly these surveys revealed many planetary nebulae; but other types of objects such as small diffuse nebulae were sometimes included. The work of Westerlund & Smith (1964) and Henize & Westerlund (1963) appears to have isolated a group of objects in the Clouds which are, in the main, similar to galactic planetaries (*cf.* Westerlund 1967). These objects are all too small to show a resolved disc in present telescopes. Slit spectroscopy (Feast 1964b and this paper) confirms that the majority of these objects are true planetary nebulae whilst eliminating a few objects which are not. In an earlier paper (Feast 1964b) preliminary radial velocities were listed for nine planetary nebulae in the LMC chosen to lie at each end of the major axis. The results showed that the subsystem of planetary nebulae in the LMC was in rotation and furthermore that there appeared to be no significant difference from the rotation curve defined by extreme Population I objects although the velocity dispersion was higher. In the present paper a much more extensive investigation of the radial velocities of planetary nebulae in both Magellanic Clouds is reported.

2. *Observations*

General. Objects were chosen for observation which seemed, on the basis of the existing information, to be almost certainly planetary nebulae. All the spectroscopic observations were made with the two prism spectrograph at the Cassegrain focus of the 74-in. (188-cm) reflector. Three different dispersions were used; the *c* camera (*f*/3·7) 49 Å/mm at Hγ (48 plates used), the *d* camera (*f*/2) 86 Å/mm at Hγ (43 plates used) and the *e* camera (*f*/1) 170 Å/mm at Hγ (19 plates used). As will be shown later the *c* camera results have by far the greatest weight in the radial velocity determinations and only 4 of the 36 objects finally adopted as planetaries were not observed at least once with this camera. However, the lower dispersion plates are of importance since, in general, they record more lines and the objects may be classified with greater certainty as planetary nebulae. All the spectra were measured in the usual way (direct and reversed) on a Casella projection machine against an iron arc comparison spectrum. Wavelengths of the forbidden nebular lines were taken from Bowen's work (1955) and other emission line wavelengths from the multiplet table (Moore–Sitterly, 1945). The lines measured included the Balmer lines, N_1, N_2 and 4363 (of [O III]) and [Ne III], He I and He II lines. For the iron arc lines the usual practice has generally been followed of adopting IAU recommended lines and wavelengths. However, to enable the use of the nebular lines N_1 and N_2 with the *c* camera, the iron arc was exposed somewhat more densely

Downloaded from https://academic.oup.com/mnras/article/140/3/345/2602684 by guest on 20 August 2022

© Royal Astronomical Society • Provided by the NASA Astrophysics Data System

1968MNRAS.140..345F

than usual and a considerable number of additional lines measured in the 5000 Å region. The wavelengths of these lines were taken from the M.I.T. Tables (Harrison 1939) and provided a good correction curve in this wavelength region.

Systematic errors for the c camera. The *c* camera has been used extensively over the past 15 years for radial velocity work and the results for standard stars found to agree well with the system of the General Catalogue of Radial Velocities. It happens however, that in the measurement of standard and programme stars, rather little weight is generally contributed to the mean by Hβ or other lines in this region; the bulk of the weight, in most work, being provided by lines at shorter wavelengths (e.g. the Hγ region). Since N_1, N_2 (5007, 4959 Å) and Hβ are often the strongest lines on the present plates, they have considerable weight, especially in the *c* camera work where relatively few lines tend to be recorded. It is therefore desirable to check these lines for possible systematic errors. Fifteen *c* camera spectra were chosen on which a good measure of at least Hγ had been obtained in addition to N_1, N_2 and Hβ. The mean differences and their standard errors are:

$$\Delta(N_1\text{-H}\gamma) = +0{\cdot}2 \pm 2{\cdot}1 \text{ km s}^{-1},$$
$$\Delta(N_2\text{-H}\gamma) = -4{\cdot}0 \pm 3{\cdot}0 \text{ km s}^{-1},$$
$$\Delta(\text{H}\beta\text{-H}\gamma) = +3{\cdot}7 \pm 2{\cdot}4 \text{ km s}^{-1}.$$

In view of the standard errors quoted it is unlikely that any of these residuals are significant and furthermore it will be noted that the mean residual for the three lines is zero. No systematic corrections have therefore been applied. Some check on the consistency of the *c* camera velocities is provided by a comparison of velocities of the same object observed with the telescope East and West of the piers. Some sources of error are expected to reverse sign with the reversal of the telescope. For 15 *c* camera spectra of six Magellanic Cloud planetaries one obtains Δ (West–East) $= +2{\cdot}1 \pm 2{\cdot}8$ (s.e.) km s^{-1}. Δ is thus not significantly different from zero.

Systematic errors for the d camera. In the case of the *d* and *e* cameras, the N_1 and N_2 lines are often rather overexposed. Furthermore the focus is falling off at these wavelengths on these cameras and the iron arc correction curve is somewhat uncertain. It was therefore decided to omit these lines. Hβ has been retained. For these cameras, systematic errors in the mean velocities have also to be considered. Previous investigations suggested that a correction of $+10$ km s^{-1} was necessary to *d* camera velocities of stars at the declination of the Magellanic Clouds (Feast & Thackeray 1963) possibly a result of guiding errors and the effects of atmospheric dispersion at the slit widths used with the *d* and *e* cameras (0·20 mm). In agreement with this result, no systematic errors were detected in work on extended emission nebulae (Feast 1961). This is supported by a comparison of a few additional *d* camera observations of extended emission nebulae in the Clouds with high dispersion (coudé) results (unpublished). Further evidence that no systematic corrections are necessary for *d* camera observations of extended sources is provided by measures in many of the present spectra of mercury lines scattered by the atmosphere from artificial lighting. For 49 measures of mercury lines on 31 *d* camera spectra one obtains a mean ' mercury ' velocity of $+1{\cdot}8 \pm 1{\cdot}4$ (s.e.) km s^{-1}. A result which is clearly insignificantly different from zero. Furthermore, there is no signifi-

Downloaded from https://academic.oup.com/mnras/article/140/3/345/2602684 by guest on 20 August 2022

© Royal Astronomical Society • Provided by the NASA Astrophysics Data System

1968MNRAS.140..345F

cant difference between the ' mercury ' velocities obtained East and West of the piers.

The result, quoted above, for stars cannot be adopted without test for the planetaries, although these all appear stellar, partly because these are emission objects (though it is perhaps unlikely that this could cause trouble) and partly because these objects are much fainter, visually, (15 to 16 magnitude) than the stars previously observed. The objects were in fact usually very difficult to see on the spectrograph slit and guiding procedure, and any consequent errors may well be systematically different from the previous stellar work. Of the Magellanic Cloud planetaries observed in the present programme 32 have been observed with both the *c* and *d* cameras (48 *c* camera spectra and 39 *d* camera spectra) and these yield an estimate of any systematic difference between the two cameras. Considering the *d* plate taken East and West of the piers, separately, one finds:

$$\Delta(c\text{–}d\,(\text{East})) = +4{\cdot}3 \pm 1{\cdot}8\ (\text{s.e.})\ \text{km s}^{-1}$$

$$\Delta(c\text{–}d\,(\text{West})) = +4{\cdot}5 \pm 3{\cdot}3\ (\text{s.e.})\ \text{km s}^{-1}.$$

The very close agreement of these two results is no doubt largely fortuitous but there appears to be no significant difference between the two sides of the polar axis in this work. Although the error found is of the same sign as that found previously for stars it seems to be significantly smaller. In Table I a uniform correction of $+4$ km s^{-1} has been applied to all the *d* camera velocities. This correction is relatively small and its effect on the mean velocities is very much smaller.

Systematic errors for the e camera. For six objects, for which a comparison of high weight can be obtained (12 *c* camera spectra and 9 *e* (east) camera spectra) one obtains $\Delta(c\text{–}e(\text{east})) = +19 \pm 4$ (s.e.) km s^{-1}. Only two objects are available for a comparison west of the pier. These give values for $\Delta(c\text{–}e(\text{west}))$ of $+11$ km s^{-1} and -18 km s^{-1} i.e. a mean value of -3 km s^{-1}. This value is obviously quite uncertain. It is however reinforced to some extent by observations of diffuse nebulae in the Magellanic Clouds with the *e* camera. For these objects, in each case, that can be compared with high dispersion (coudé) velocities, *d* camera velocities or the velocities of Bok *et al.* (1964) one obtains $\Delta(e(\text{east})) = +21$ km s^{-1}, $\Delta(e(\text{west})) = -7$ km s^{-1}. The following corrections were therefore adopted; to *e*(east) $+20$ km s^{-1}, to *e*(west) -5 km s^{-1}. Further evidence for corrections of the same sign and similar magnitude to these for extended sources is provided by the velocities measured for the terrestrial mercury lines. For 12 spectra (21 lines) taken east of the piers, a velocity of -17 ± 4 km s^{-1} is obtained whilst 5 spectra (9 lines) taken west of the piers give a mean velocity of $+13 \pm 9$ km s^{-1}. It should be emphasized that the considerable uncertainties in these corrections have little effect on the final results since, as will be shown below, the *e* camera results receive little weight. In fact the average change in the mean velocities made by the *d* and *e* camera corrections is $+1{\cdot}5$ km s^{-1} for the LMC and $+2{\cdot}7$ km s^{-1} for the SMC.

The observational velocity dispersion. To obtain the best mean velocities as well as to calculate the part of the velocity dispersion resulting from observational errors (Section 4), it is necessary to estimate the relative weights of the velocities obtained with different cameras. In doing this, account has been taken of the fact that for

Downloaded from https://academic.oup.com/mnras/article/140/3/345/2602684 by guest on 20 August 2022

© Royal Astronomical Society • Provided by the NASA Astrophysics Data System

1968MNRAS.140..345F

TABLE I

Radial velocities of planetary nebulae in the Magellanic Clouds

(1) Designation. For the LMC:

L = Lindsay & Mullan (1963) number;
W = Westerlund & Smith (1964) number;
H = Henize (1956) number;

For the SMC:

L = Lindsay (1961) number;
W = Classification by Henize & Westerlund (1963);
St = Stellar (i.e. probable planetary),
DN = Diffuse nebula,
OR = Outside the region they surveyed,
BL = Below magnitude limit of their survey.
H = Henize (1956) number.

(2) Date of observation.
(3) Radial velocity.
(4) Number of lines measured, camera used, telescope East or West of piers.
(5) Weight of velocity.
(6) Magnitude (B^N = Integrated blue magnitude, of Westerlund & Smith (1964) for the LMC, m_{pg} of Lindsay (1961) for the SMC) excitation class (See Section 6)
R = Remark at end of Table.

(a) Large Magellanic Cloud

Designation L	W	H	Date (U.T.)	Velocity (km s^{-1})	No. of lines and camera Tel. E, W	Weight	Magnitude excitation class remark
2	1	N182	64.10.29	+220	8dE	8	$16^m.05$
			65.10.27	+214	4cE	24	3
			65.12.25	+220	5cE	24	
			66.12.30	+223	5cE	24	
				+219		80	
4	2	N184	64.1.22	+274	8dE	8	$17^m.05$
			66.9.26	+270	3cE	24	7
				+271		32	
13	6	N188	64.10.31	+239	7dE	8	$17^m.06$
			65.12.13	+239	6cE	24	7
				+239		32	
16	7	N97	64.11.12	+248	7dE	8	$16^m.60$
			65.9.27	+251	3cW	12	8
				+250		20	
17	8	N24	65.1.5	+287	6dE	8	$16^m.73$
			65.12.25	+311	2cE	12	(3)
				+302		20	
20	10	N192	65.1.8	+267	6dE	8	$17^m.19$
			67.1.8	+240	5cE	24	8+
				+247		32	
25	15	N110	65.2.5	+238	7dE	8	$16^m.43$
			66.1.8	+244	3cE	24	—
				+243		32	

Downloaded from https://academic.oup.com/mnras/article/140/3/345/2602684 by guest on 20 August 2022

© Royal Astronomical Society • Provided by the NASA Astrophysics Data System

1968MNRAS.140..345F

TABLE I (*continued*)

Designation L	W	H	Date (U.T.)	Velocity (km s^{-1})	No. of lines and camera Tel. E, W	Weight	Magnitude excitation class remark
28	18	N122	65.2.24	+296	7dE	8	$15^{m}.74$
			67.1.14	+261	1cE	12	8
				+275		20	
31	20	N39	64.2.18	+337	6dE	8	$16^{m}.69$
							5
				+337		8	
33	21	N124	65.3.1	+265	9dE	8	$16^{m}.22$
			65.12.16	+289	2cE	12	6
				+280		20	
34	22	N42	64.2.8	+288	8dE	8	$16^{m}.52$
			65.10.2	+270	2cW	12	4
				+277		20	
35	—	N44A	64.2.23	+293	8dE	8	—
							2−1
							R
				+293		8	
37	24	N203	61.10.8	+186	1dW	4	$16^{m}.48$
			61.11.2	+198	10eE	2	(3)
			62.12.7	+182	3dE	8	R
			63.12.18	+183	3dE	8	
				+185		22	
42	27	N52	64.3.14	+308	6dE	8	$17^{m}.00$
			66.3.18	+308	3cE	24	5
				+308		32	
45	29	N208	65.3.28	+235	7dE	8	$15^{m}.93$
			65.10.16	+242	9cW	24	5+
			65.11.17	+236	4cE	24	
				+239		56	
49	33	N153	64.3.17	+225	4dE	8	$15^{m}.73$
			65.12.7	+260	9cE	24	5
				+252		32	
50	—	N210	61.11.30	+201	4eE	2	—
			61.12.5	+241	6eE	2	(4−5)
			61.12.27	+254	6eE	2	
			63.2.14	+232	2dE	4	
			63.3.1	+260	2dE	8	
			67.3.4	+219	3cE	24	
				+230		42	
51	34	N211	64.1.12	+235	8dE	8	$16^{m}.48$
			65.12.20	+234	4cE	24	4
				+234		32	
52	35	N66	64.12.25	+302	2dE	4	$15^{m}.76$
			65.11.19	+279	1cE	12	(2?)
			65.12.4	+290	1cE	12	
				+287		28	

Downloaded from https://academic.oup.com/mnras/article/140/3/345/2602684 by guest on 20 August 2022

© Royal Astronomical Society • Provided by the NASA Astrophysics Data System

1968MNRAS.140..345F

TABLE I (*continued*)

Designation L	W	H	Date (U.T.)	Velocity (km s^{-1})	No. of lines and camera Tel. E, W	Weight	Magnitude excitation class remark
53	36	N212	65.1.8	+258	2dE	4	16^{m}.72
			66.3.12	+262	4cE	24	(3?)
				+261		28	
55	37	N215	65.1.5	+317	4dE	4	17^{m}.00
			65.12.14	+278	3cE	24	9
				+284		28	
56	38	N178	64.11.9	+271	10dE	8	15^{m}.92
			65.10.23	+278	8cW	24	5
				+276		32	
58	39	N170	64.10.26	+254	9eE	2	15^{m}.80
			64.11.27	+268	7dE	8	7
			65.12.10	+278	4cE	24	
				+274		34	
61	40	—	65.2.5	+288	2dE	4	16^{m}.3
			67.1.9	+294	2cE	12	9
				+293		16	
62	41	—	65.1.3	+258	5dE	8	16^{m}.13
			66.1.10	+264	6cE	24	—
				+262		32	
63	42	N221	64.3.19	+258	2dE	4	16^{m}.05
			64.3.25	+266	8dE	8	5
			64.4.2	+258	8dE	8	
			64.4.6	+255	8dE	8	
			66.3.28	+260	4cE	24	
			66.4.16	+271	4cE	24	
				+263		76	
			(b) Small Magellanic Cloud				
14	OR	N2	64.7.14	+160	9eE	2	16^{m}.39
			64.10.28	+161	8dE	8	6
			65.8.20	+163	5dW	8	
			65.9.5	+161	6cE	24	
			66.6.20	+150	5cW	24	
			66.7.7	+155	4cW	24	
				+157		90	
32	BL	N5	64.7.18	+93	6eE	2	16^{m}.35
			64.11.8	+116	8dE	8	8–
			65.8.18	+103	7dW	8	
			65.10.16	+118	6cW	24	
			66.7.11	+101	5cW	24	
				+109		66	
33	St	N6	64.8.10	+137	4eW	2	16^{m}.46
			65.7.28	+130	4dE	8	(3)
			65.10.22	+162	3cW	24	
			66.7.13	+144	4cW	24	
				+149		58	

Downloaded from https://academic.oup.com/mnras/article/140/3/345/2602684 by guest on 20 August 2022

© Royal Astronomical Society • Provided by the NASA Astrophysics Data System

1968MNRAS.140..345F

TABLE I (*continued*)

Designation L	W	H	Date (U.T.)	Velocity (km s^{-1})	No. of lines and camera Tel. E, W	Weight	Magnitude excitation class remark
43	BL	N7	64.8.7	+142	2eW	1	16^{m}·38 (2)
				+142		1	
144	St	N38	64.8.16	+168	7eE	2	16^{m}·01 (3)
			65.7.10	+165	7dW	8	
			65.9.21	+158	4cE	24	
			66.8.24	+160	5cE	24	
				+160		58	
174	St	N43	64.8.8	+115	5eE	2	15^{m}·96 (2)
			65.8.7	+113	6eE	2	
			65.8.10	+109	5dE	8	
			65.8.23	+116	3dW	8	
			65.9.1	+118	4cW	24	
			66.8.22	+114	4cE	24	
				+115		68	
191	St	N44	64.8.15	+125	4eW	2	15^{m}·98 (4)
			64.11.26	+114	5dE	8	
			65.9.2	+113	7cE	24	
			65.10.5	+114	5cW	24	
			65.12.7	+112	4cE	24	
			65.12.10	+112	4cE	24	
				+113		106	
275	St	N55	64.8.30	+168	4eW	2	15^{m}·71 — R
				+168		2	
289	OR	N54	64.8.31	+96	8eE	2	16^{m}·0 1
			65.8.19	+101	5dE	8	
			65.9.20	+106	5cW	24	
			66.9.8	+92	4cE	24	
				+99		58	
333	BL	N67	65.8.6	+113	3eE	2	16^{m}·69 —
				+113		2	
339	DN	N68	64.9.4	+119	2eE	1	15^{m}·71 0 R
			64.12.25	+138	2dE	4	
				+134		5	
347	St	N70	64.9.7	+112	3eE	1	16^{m}·07 1
			65.1.3	+151	2dE	4	
			65.9.26	+150	4cW	24	
				+148		29	
532	St	N87	64.8.11	+86	2eE	1	15^{m}·94 2
			64.10.30	+110	9dW	8	
			65.12.19	+120	5cE	24	
			66.9.7	+117	4cW	24	
				+117		57	

Downloaded from https://academic.oup.com/mnras/article/140/3/345/2602684 by guest on 20 August 2022

© Royal Astronomical Society • Provided by the NASA Astrophysics Data System

1968MNRAS.140..345F

Remarks to Table I:

Large Magellanic Cloud

$L35 = N44A$. Discussed by Feast (1964b) and considered to be a high excitation diffuse nebula rather than a planetary despite the planetary classification of Lindsay & Mullan (1963) and of Westerlund & Rodgers (1959). Apparently also rejected as being non-planetary by Westerlund & Smith (1964).

$L37 = N203$. 4650A C III detected from the central star. 3726[O II] $\gg$ 3729[O II] indicating high electron density ($\sim 2 \times 10^4$ electrons cm^{-3}) (*cf.* Feast 1964b).

Note. I am indebted to Dr B. E. Westerlund for confirming that the identification chart for this object in Westerlund & Smith (1964) is incorrect. Henize (1956) correctly identifies the object.

$L58 = N170$. 3726[O II] $\gg$ 3729[O II] indicating high electron density.

Small Magellanic Cloud

$L14 = N2$. 3726[O II] $\gg$ 3729[O II] indicating high electron density.

$L144 = N38$. 3726[O II] probably stronger than 3729[O II].

$L275 = N55$. Not a planetary, see Section 5, paragraph 1. The velocity depends on the [Fe II] lines 4244, 4277, 4287, 4359A.

$L339 = N68$. Not a planetary, see Section 5 paragraph 1.

each camera a few spectra of poorer quality have been assigned half weight. From the 12 objects (28 spectra) with more than one *c* camera spectrum each, the standard error of a *c* camera spectrum of full weight is found to be $\sigma_c = 6{\cdot}3 \pm 1{\cdot}1$ km s^{-1}. From 32 objects with both *c* and *d* plates and six objects with two or more *d* plates (15 plates), the standard error of a *d* camera velocity of full weight is found to be $\sigma_d = 11{\cdot}2 \pm 1{\cdot}4$ km s^{-1}. Since the weights are inversely proportional to the squares of the standard errors, it follows that the weights of the *c* and *d* velocities are in the ratio of about 3 to 1. A similar ratio was found by Wesselink (unpublished) for stars in the Magellanic Clouds observed with these two cameras. From 11 objects with both *c* and *e* camera plates, the standard error of an *e* camera velocity of full weight is found to be $\sigma_e = 19{\cdot}9 \pm 4{\cdot}0$ km s^{-1}. These results lead to the weighting system listed below, where colons denote half weight objects. With this weighting system and using all the available planetaries a standard error for an observation of unit weight is found to be 31·8 km s^{-1}. The corresponding standard errors for objects of other weights are shown in the table.

Camera	Weight	Standard error (km s^{-1})
c	24	6·5
c:	12	9·2
d	8	11·2
d:	4	15·9
e	2	22·5
e:	1	31·8

Table I contains the individual radial velocities, the *d* and *e* camera results corrected according to the results outlined above. The means were determined according to the weighting system just discussed. It should be noted that because all the work was originally carried out to the nearest 0·1 km s^{-1} and only rounded off in forming Table I for printing, there may occasionally be a slight apparent inconsistency between the mean given and the individual values. Some remarks

Downloaded from https://academic.oup.com/mnras/article/140/3/345/2602684 by guest on 20 August 2022

© Royal Astronomical Society • Provided by the NASA Astrophysics Data System

1968MNRAS.140..345F

on individual objects follow the table. For a few of the objects in Table I, preliminary velocities were published previously (Feast 1964b). The present results supersede these preliminary values which were based on part of the present material.

As noted in the remarks a few of the objects in Table I are not planetary nebulae. The excitation classes found for the rest of the objects which will be discussed in Section 6 point strongly to their being planetary nebulae. Furthermore, as shown in the remarks to Table I a few objects have spectra sufficiently well exposed that the [O II] doublet 3726/3729 is recorded. The relative intensities of these two lines indicate high densities for these objects consistent with their classification as planetaries (cf. Feast 1964b). In one case (Henize LMC N203) a broad emission band arising from the nuclear star was detected.

3. *Rotation of the planetary nebula subsystem in the LMC.* In the present section the velocities of the 25 LMC objects in Table I adopted as planetaries will be discussed for the rotation of the subsystem of planetaries in the LMC. As in previous work on the LMC (Feast, Thackeray & Wesselink 1961; Feast 1964a) the velocities were corrected for a solar motion of 20 km s^{-1} towards $\alpha = 18^h$ $\delta = 30°$ (1900) and a galactic rotation term of 270 km s^{-1} towards $l^{II} = 57°$ $b^{II} = 0°$. The conclusions are quite insensitive to the actual values of the solar motion and galactic rotation that are adopted.

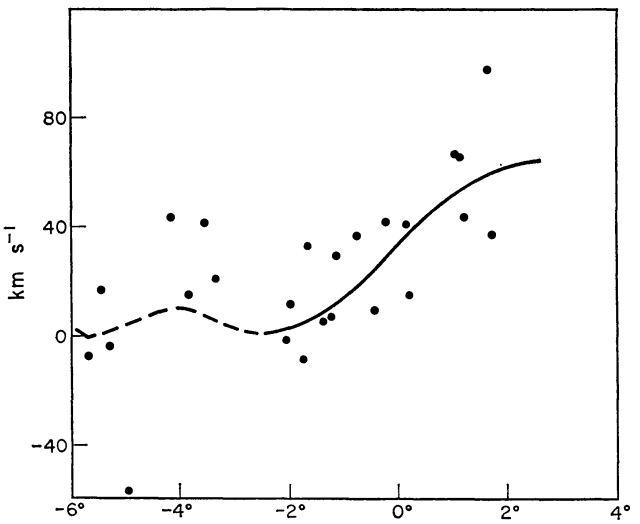

FIG. 1. *The rotation of the subsystem of planetary nebulae in the LMC. Ordinate: radial velocities (km s^{-1}) corrected for solar motion and galactic rotation. Abscissa: angular distance along p.a. 171° (Northern side of centre is positive). The points are planetary nebulae. The curve is derived from extreme Population I objects.*

The extreme Population I objects (supergiant stars, diffuse nebulae and interstellar gas) show quite clearly the effects of differential rotation of this young subsystem of the LMC (Feast 1964a; McGee & Milton 1966). They indicate the direction of maximum velocity gradient to be in position angle 171°. In Fig. 1 the velocities of the planetaries, corrected for solar motion and galactic rotation are plotted against angular distance along this position angle. The Population I rotation curve (Feast 1964a, Fig. 1) is shown. In this plot 0° corresponds to the centre of symmetry of the Population I rotation curve which is displaced 1° north of the main optical bar. The dotted extension to the rotation curve is taken from

Downloaded from https://academic.oup.com/mnras/article/140/3/345/2602684 by guest on 20 August 2022

© Royal Astronomical Society • Provided by the NASA Astrophysics Data System

1968MNRAS.140..345F

the 21 cm work (McGee & Milton 1966) and must be considered somewhat uncertain as a result of the complexity of the 21 cm results. An examination of this plot reveals no good evidence for any systematic deviation between the systematic motions of the planetaries and extreme Population I objects. Certainly in the central region $\pm 2°$ where the young optical objects give a well defined curve, the agreement with the planetaries is very satisfactory.

Since differential rotation is present, further progress can only be made by adopting a model for the system. As previously, we adopt de Vaucouleurs' model (1960) of a system flattened to a plane inclined at an angle $i = 27°$ to the plane of the sky. Proper projection factors may then be applied to the observed radial velocities and angular distances from the centre of rotation to obtain a rotation curve in the plane of the system. Fig. 2 shows the LMC planetaries plotted in this

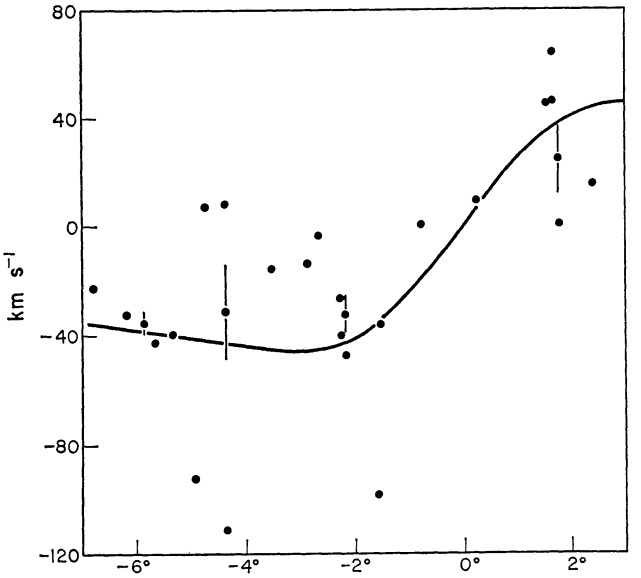

FIG. 2. *The rotation of the subsystem of the LMC planetaries in the inclined plane model. Ordinate: V sin i, where V is the radial velocity projected into the plane of the system and i = 27° (the adopted inclination of the LMC). Abscissa: angular distance from the centre of rotation measured in the plane of the system (Northern side of the centre is positive). The four points with vertical standard error bars are mean points for planetary nebulae. The other points are individual planetaries. The curve is the Bottlinger type rotation curve derived from extreme Population I objects.*

way (if V is the rotation velocity in the plane of the system, the figure shows $V \sin i$ plotted against true angular distance from the centre of rotation). Fig. 2 also shows the Bottlinger type rotation curve determined previously from the optical work on extreme Population I objects (Feast 1964a). Because of the differing projection factors the points in Fig. 2 have a very wide range of weights (and in fact two points of very low weight are omitted in this plot). A comparison with the curve is therefore best made using weighted mean points. The weights of the individual points depend on the projection factors and also on the accuracy of the measured velocity. Since much of the observed dispersion is a result of a real (cosmic) velocity dispersion rather than purely observational scatter (see Section 4) it is not appropriate to use the weights of individual mean velocities given in Table I. In this section of the work the mean radial velocities were assigned a weight of 1 or 2 depending on whether the weight in Table I was greater or less than 18. The four

Downloaded from https://academic.oup.com/mnras/article/140/3/345/2602684 by guest on 20 August 2022

© Royal Astronomical Society • Provided by the NASA Astrophysics Data System

1968MNRAS.140..345F

weighted mean points are shown, with vertical bars corresponding to their standard errors, in Fig. 2. It has to be recognized that there is some considerable uncertainty in the curve shown in Fig. 2. For one thing, it represents a forced fit of the young LMC objects to a Bottlinger type model and we do not know how closely the LMC actually approximates to such a model. In view of this it is extremely doubtful whether one should take the relatively small deviations of the mean points from the curve at all seriously especially since they are hardly outside the standard errors of the planetary points. Nevertheless if these deviations were taken seriously they would indicate a somewhat shallower rotation curve for the planetaries but still about the same centre of rotation. Such an effect for a subsystem such as the

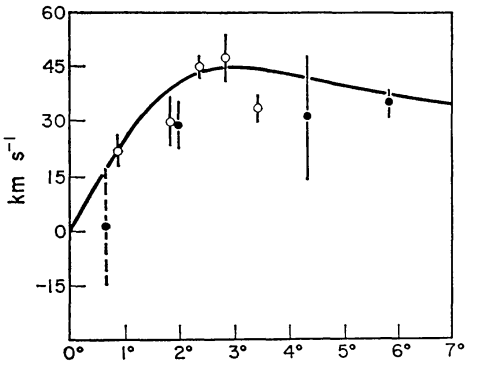

FIG. 3. *As Fig. 2 but with objects on both sides of the centre of rotation combined. Filled circles are mean points for planetary nebulae. Open circles are mean points for extreme Population I objects. The curve is the best fit of a Bottlinger type curve to the open circles. The vertical lines indicate the standard errors of the points.*

planetaries with somewhat higher velocity dispersion than the younger objects (see Section 4) would not be at all unreasonable *a priori* (it is the equivalent of the asymmetrical drift in the Galaxy). However, Fig. 3 shows that there are probably no firm grounds for making such an interpretation. This figure is the same as Fig. 2 except that the results have been reflected in the centre of rotation. The filled circles are the mean points for the planetary nebulae and the open circles are the mean Population I points from which the Bottlinger curve was derived (Feast 1964a, Fig. 3). Standard errors are shown (in the case of the point at $r = 0°{\cdot}7$ only two planetaries are used in the mean and the dotted line indicates a standard error for a mean of the correct weight estimated from the whole body of data). It will be seen that the only apparently significant deviation of the planetaries from the Bottlinger curve is near $r = 2°$, but it is striking that at this value of r the extreme Population I mean point also deviates by the same amount from the curve. It may be concluded therefore from this discussion of both the direct plot (Fig. 1) and the inclined plane model (Figs 2 and 3), that not only is the subsystem of planetary nebulae in the LMC in rotation but also that (contrary to the conclusions of Webster (1965)) the rotational velocities of the planetaries are in good agreement with those of the extreme Population I objects.

These conclusions have a number of important consequences. It has been known for some while that the centre of rotation deduced from young objects is displaced 1° (~ 1 kpc) North of the main optical bar of the LMC. Furthermore the surface distributions of these young objects also have centres of symmetry

Downloaded from https://academic.oup.com/mnras/article/140/3/345/2602684 by guest on 20 August 2022

© Royal Astronomical Society • Provided by the NASA Astrophysics Data System

1968MNRAS.140..345F

displaced 1° north of the bar. This apparent lack of any effect of the LMC bar on the distribution and motions of the young objects was puzzling and might indeed have been taken as a point in favour of the interpretation of the LMC as two virtually independent systems (a young system plus an old (bar) system) seen in the same line of sight, an idea put forward originally by Johnson (1959). However, the planetary nebulae are distributed (Westerlund & Smith 1964) symmetrically about a point near the optical centre (essentially the centre of the bar system). Evidently the planetaries appear to be spatially related to the bar system rather than to the young system. But, since the overall rotational pattern of the planetaries is the same as that of the young objects, it must be concluded that we are dealing with one single (complex) system.

In spite of the irregular barred appearance of the LMC, the rotation curve for young objects (Feast 1964a, Fig. 1) is strikingly smooth and symmetrical. This, in itself, would seem to imply circular motions in a system with its mass centre at the centre of rotation. There are clearly formidable difficulties in displacing the centre of mass so far from the optical bar where one might reasonably suppose the centre of mass to be. These difficulties are not made lighter by the discovery that some other systems show a similar displacement of the centre of rotation from the optical centre. Two possible solutions to the problem have been proposed. Wesselink (1966) suggests that there is a large amount of obscuration north of the LMC bar where the true mass centre lies, whilst Bolton (1965) suggests the presence in this region of large amounts of matter in an undetected form such as H_2. A direct observational check on at least the former hypothesis seems possible. Indeed the fact that infra-red photography (Johnson 1959) does not reveal a northern extension to the bar region may perhaps be taken as evidence against such an hypothesis. If on the other hand it is maintained that the optical bar is a real, rather than an apparent feature of the LMC mass distribution, then the displacement of the rotational centre would have to be regarded as a result of the disturbing effects of non-circular motions in a barred system (an approach advocated by de Vaucouleurs (1964)). In view of the considerable complexity revealed by the recent 21 cm studies (McGee & Milton 1966a, b) this latter suggestion would be worth investigating in some detail using all the available optical and radio data. Since all the evidence points to the LMC planetaries being old objects (see Section 4), the present results show that if non-circular motions exist then they must apply to objects of a wide range of ages. The overall kinematical pattern that has been found appears to be a fundamental property of the LMC rather than a peculiarity confined to its very youngest members.

4. *The velocity dispersion and age of LMC planetaries.* The velocity dispersion for the planetary nebulae in the LMC was calculated from the residuals of the observed velocities from velocities predicted by the Bottlinger interpolation formula (Feast 1964a). The value obtained, 22·6 km s^{-1}, is not appreciably different from that obtained using residuals from the Population I curve in the direct plot (Fig. 1), 21·9 km s^{-1}. A correction for observational error was applied using the standard method (Trumpler & Weaver 1953). The weights of the planetaries were those given in Table I and the standard error of an observation of unit weight derived in Section 2 was used. The velocities are sufficiently accurate that the correction for observational dispersion is very small. The uncorrected dispersion of 22·6 km s^{-1} reduces to 21·8 km s^{-1}. A mean true velocity dispersion of 22 ± 3 (s.e.)

Downloaded from https://academic.oup.com/mnras/article/140/3/345/2602684 by guest on 20 August 2022

© Royal Astronomical Society • Provided by the NASA Astrophysics Data System

1968MNRAS.140..345F

km s^{-1} has been adopted for the LMC planetaries. This result happens to be precisely the same as that obtained previously (Feast 1964b) from a much smaller body of data (22 ± 7 (s.e.) km s^{-1}) though the standard error is now considerably reduced.

The velocity dispersion obtained for the planetaries is significantly larger than that obtained for young objects, $9{\cdot}6 \pm 1{\cdot}1$ km s^{-1} (Feast 1964a). In the de Vaucouleurs model the plane of the LMC makes an angle of only 27° with the plane of the sky, thus the motions perpendicular to the plane (z motions) are quite close to the line of sight. In this model therefore, the observed velocity dispersion is mainly a result of z motions. It seems rather unlikely, in any case, that the velocity dispersion of the planetaries in the plane of the LMC could increase substantially over that of the extreme Population I objects without increasing the z dispersion also. Thus it would appear quite safe to deduce from the present results that the z dispersion of the LMC planetaries is higher than that of extreme Population I objects.

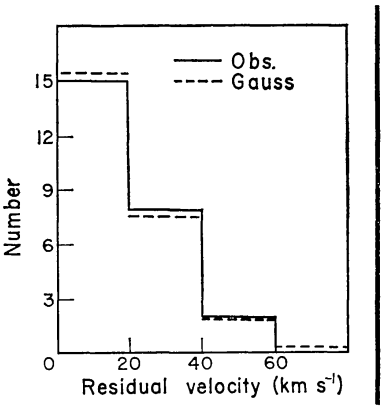

FIG. 4. *Distribution of the velocity residuals from the predictions of the Bottlinger model for the LMC planetaries. The observed distribution is given by the full line whilst the dotted line indicates the best gaussian fit to the distribution.*

A histogram of the observed velocity residuals is shown in Fig. 4 together with the theoretical gaussian fit (for the observed dispersion of 22·6 km s^{-1}). Clearly the residuals fit a gaussian distribution very well. Webster (1965), (see also Westerlund (1967)), has noted, in analysing some earlier results, that if the planetaries with large residuals are omitted the velocity dispersion can be brought down to a value similar to that of the young objects. The excellence of the gaussian fit in Fig. 4 however, suggests that there is little justification at present for subdividing the material in this way. It is of course true that in the Galaxy the planetaries cover a relatively wide range of ages and require subdividing into groups of similar age each with its own velocity dispersion. A similar situation may exist in the LMC. However, the velocities so far available do not force such a conclusion and any attempt to subdivide the LMC planetaries must at the present time use other criteria. The number of planetaries observed is as yet, unfortunately, too small for any highly significant results to be obtained by subdividing the data. Nevertheless, two points are worthy of note.

Firstly, there is no striking change in velocity dispersion from the centre to the edge of the LMC. If anything, the dispersion may be slightly greater in the outer parts but this is quite uncertain. In the Galaxy there is a very marked increase

Downloaded from https://academic.oup.com/mnras/article/140/3/345/2602684 by guest on 20 August 2022

© Royal Astronomical Society • Provided by the NASA Astrophysics Data System

1968MNRAS.140..345F

in velocity dispersion as the centre is approached. This has been taken to indicate a decreasing mean age for the galactic planetaries with increasing galacto-centric distance (Feast 1966). In considering this difference between the Galaxy and the LMC one must remember that there is no marked central condensation of the planetaries in the LMC (see Westerlund & Smith (1964) and Fig. 5 of the present paper) in contrast to the state of affairs in the Galaxy.

Secondly, there is a slight indication that the fainter LMC planetaries have a higher velocity dispersion than the brighter ones. A plot suggests a division near $16^{m}\cdot4$ (the B^N magnitudes of Westerlund & Smith (1964)) and this conveniently divides the material in half. The results for the corrected velocity dispersions are:

(1) fainter than $B^N = 16^{m}\cdot4$, 13 objects, corrected dispersion 27 ± 6 (s.e.) km s^{-1};

(2) brighter than $B^N = 16^{m}\cdot4$, 11 objects, corrected dispersion 15 ± 4 (s.e.) km s^{-1}.

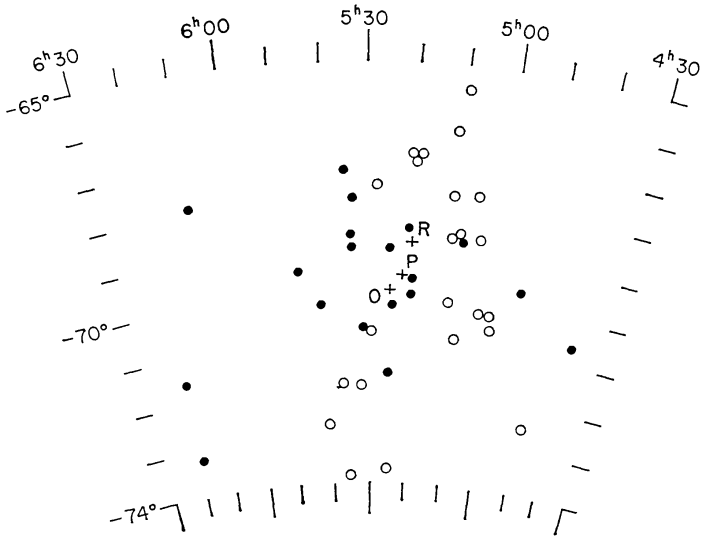

FIG. 5. *Surface distribution of LMC planetaries according to Westerlund & Smith* (1964). *Those fainter than* $B^N = 16^{m}\cdot4$ *are open circles.* R = *centre of rotation,* P = *centroid of planetary nebulae,* O = *geometric centre of core.*

Only 24 of the 25 planetaries could be used for this comparison since for one object no B^N value is available. In neither group are there significant deviations from a gaussian distribution. However, the numbers are extremely small for this type of test. The result is suggestive but naturally requires confirmation. It will be seen that the dispersion of the brighter objects may not differ significantly from that of extreme Population I objects. It is of interest in this connection to study the surface distribution of the planetaries. Fig. 5 shows this distribution according to Westerlund & Smith (1964) except that in this plot the bright and faint planetaries are plotted with different symbols. There is certainly a suggestion that the fainter planetaries are somewhat differently distributed from the bright ones. They seem to show a markedly elongated distribution. The major axis of this distribution coincides with the major axis of rotation. However, it is not immediately clear how the suggested differences in the velocity dispersions and the space distributions can be reconciled.

As was noted in the introduction, the planetary nebulae in the Galaxy, although encompassing a wide range of ages, are all old objects. The photometric (Westerlund

Downloaded from https://academic.oup.com/mnras/article/140/3/345/2602684 by guest on 20 August 2022

© Royal Astronomical Society • Provided by the NASA Astrophysics Data System

1968MNRAS.140..345F

1967) and spectroscopic evidence, (this paper) shows the close general similarity of the planetaries in the Magellanic Clouds to those in the Galaxy and strongly indicates that these are, similarly, old objects. Additional evidence that the LMC planetaries are of quite a different age from the extreme Population I objects is given by the results on the surface distribution of the various objects. As discussed in Section 3 the centre of symmetry of the planetaries is quite different from that of the extreme Population I objects. Furthermore, although it was shown in Section 3 that the overall rotational pattern for the planetaries is the same as that for extreme Population I objects, it has just been shown that the mean velocity dispersion for the planetaries is considerably higher than for the extreme Population I objects. This is also shown in a slightly different way by the lack of detailed correlation between the positions and velocities of the planetaries and the velocities and densities of the interstellar gas as determined from 21 cm observations. McGee (1964) and McGee & Milton (1966a) have shown that there is a very close detailed correlation between the velocities of young objects (supergiant stars and diffuse nebulae) and the velocities and densities of the interstellar gas. McGee & Milton (1966a) used some preliminary velocities of LMC planetaries (Feast 1964b) to show that no such close correlation exists in this case. The much more extensive results of Table I have been compared with the 21 cm results in the same way. This is best done by plotting the velocities and positions of the planetary nebulae on the velocity–intensity–position diagrams of McGee & Milton (1966b) (their Figs 1–67). Such a comparison shows little evidence of any detailed correlation between the interstellar gas and the planetaries. For instance, of the 25 LMC planetaries, nine fall outside the lowest intensity contours of the 21 cm plots (i.e. below 2·5 units on the scale of McGee & Milton) whilst 19 of the 25 fall at 21 cm intensities of 10 or less which is still a low intensity. In fact of the 26 LMC objects in Table I only one (N44A) falls close to a pronounced intensity peak in the 21 cm observations and this is the one object which, on other grounds, is now considered to be a small diffuse nebula rather than a planetary (see the note to Table I). All the evidence therefore points to the planetaries in the LMC belonging to a distinctly different age group from the extreme Population I objects and, as in the case of the Galaxy, it may be inferred that they constitute an old subsystem. The higher z dispersion deduced earlier in this section for the LMC planetaries as compared with young objects gives evidence therefore that in the LMC, as in the Galaxy there has been a collapse to a plane. Further studies of planetary nebulae and other old objects in the LMC should eventually enable the kinematical and chemical history of the collapse to be explored in detail.

5. *The kinematics of the planetary nebulae in the SMC.* On the present programme radial velocities have been obtained for 13 objects originally considered to be planetary nebulae in the SMC. However Henize SMC N68 was resolved on a direct photograph by Henize & Westerlund (1963) and is considered by them to be a small diffuse nebula of about two solar masses. In agreement with this conclusion is the fact that it has been found to have the lowest excitation of any object in the present programme (see Section 6). Henize SMC N55 is an interesting object, it turns out to have [Fe II] emission and possibly TiO absorption. Clearly it is a peculiar emission line star and as such warrants further study.

Although there are only 11 planetaries in the SMC with known velocities most of these have a high weight (average standard error 4 km s^{-1}). Since it i

Downloaded from https://academic.oup.com/mnras/article/140/3/345/2602684 by guest on 20 August 2022

© Royal Astronomical Society • Provided by the NASA Astrophysics Data System

1968MNRAS.140..345F

of considerable interest to make a direct comparison between the present results and the 21 cm observations, the velocities of the planetaries have been corrected for galactic rotation and solar motion using the values employed by Hindman, Kerr & McGee (1963) and Hindman & Balnaves (1967) i.e. a solar motion of 20 km s^{-1} towards $18^h+30°$ (1900), a galactic rotation of 216 km s^{-1} and a 'Kerr' galactic expansion term of 7 km s^{-1}. The present discussion would not be affected by any reasonable changes to these values (including dropping the Kerr term).

As in the case of the LMC we can examine the velocities of the SMC planetaries for detailed correlation with the 21 cm results on the interstellar H I; the best means of comparison being with the velocity–intensity–position plots of Hindman & Balnaves (1967) (their Figs 2–50). The detailed correlation is found to be poor. Four of the 11 planetaries fall outside the lowest H I contour (below 2 units in the system of Hindman & Balnaves) whilst 9 of the 11 planetaries fall in the velocity–intensity–position plots at points of H I intensity of 10 units or less (a relatively low intensity). As in the case of the LMC this lack of correlation of the

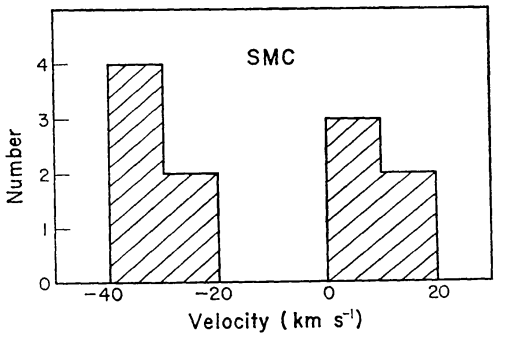

FIG. 6. *Distribution of velocities (km s^{-1}) of SMC planetaries corrected for galactic rotation and solar motion.*

planetaries with H I is made very striking by the fact that whilst the one SMC object on the present programme now classified as a diffuse nebula (N68) coincides closely in position and velocity with an intense 21 cm peak, none of the SMC planetaries give evidence for a connection with any intense 21 cm peaks. As in the case of the LMC this may be taken as evidence that these planetaries are old objects.

The most remarkable feature in the overall distribution of the planetary velocities is shown in Fig. 6. Here the residual velocities (i.e. the velocities corrected for solar motion and galactic rotation) are collected into a histogram. It will be seen that there is a clear division into two distinct groups. This does not appear to be a regional effect since in some cases planetaries of the high and low velocity groups occur relatively close together in the SMC. The two groups do not appear to be related to either excitation class (as defined in Section 6) or magnitude.

This division into two groups is very reminiscent of the double peaks which were found in the 21 cm profiles over large regions of the SMC by Hindman, Kerr & McGee (1963). Fig. 7 is adapted from their Fig. 9. It shows the 21 cm peak velocities plotted against perpendicular distance from the (arbitrary) meridian 01^h20^m. The crosses in this figure are the present planetary nebulae. The division of both the 21 cm results and the planetary velocities into two groups is clearly

Downloaded from https://academic.oup.com/mnras/article/140/3/345/2602684 by guest on 20 August 2022

© Royal Astronomical Society • Provided by the NASA Astrophysics Data System

1968MNRAS.140..345F

seen in this figure. Over the region covered by the planetary observations, the 1963 21 cm results yield fairly constant velocities for the two groups of about -14 km s^{-1} and $+14$ km s^{-1}. It is evident in Fig. 7 that the positive group of 21 cm peaks fits quite well with the positive group of planetaries. The best stellar radial velocities (young supergiant stars) seem to show a rather broad frequency distribution centred on this positive group (Thackeray, private communication). However, the negative velocity group of planetaries seems to have a systematically more negative velocity than the corresponding 21 cm peaks. Furthermore, there appears to be little or no evidence for supergiants associated with the negative

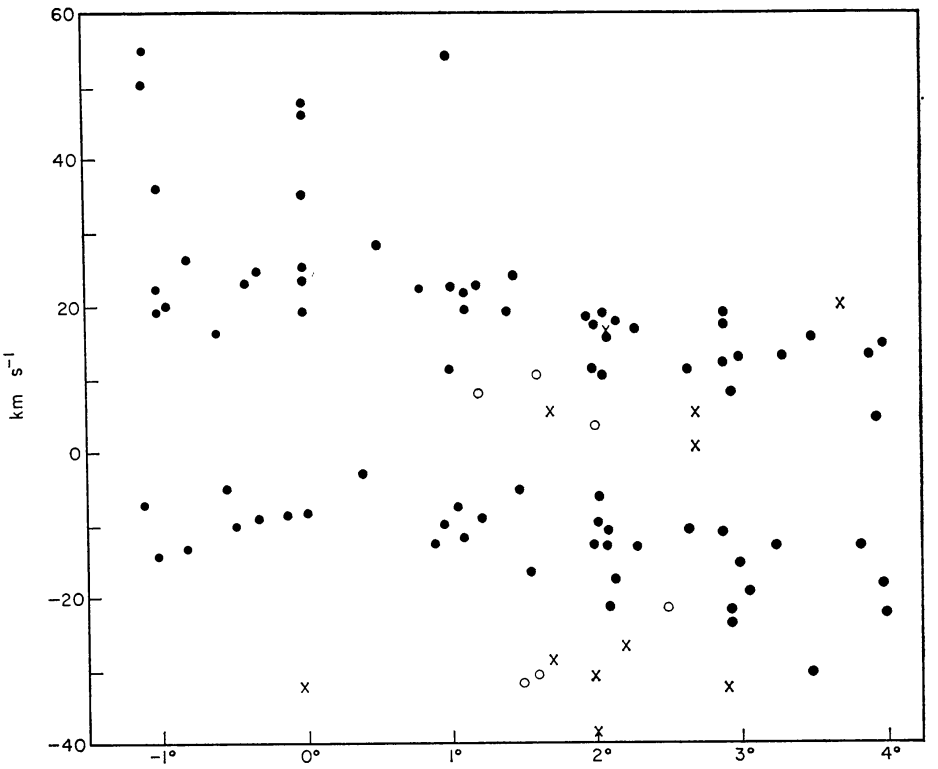

FIG. 7. *The velocity pattern across the SMC. Ordinate: velocity corrected for solar motion and galactic rotation. Abscissa: perpendicular distance (degrees) from the* 01^h20^m *meridian (preceding to the right). Filled circles are 21 cm peaks from Hindman, Kerr & McGee* (1963, *Fig.* 9). *Crosses are planetary nebulae. Open circles are Ca II interstellar velocities.*

group of the H I or of the planetaries. On the other hand optical work gives evidence for interstellar gas at the same negative velocity as the planetaries. Hindman (1964) was the first to notice that the optical interstellar Ca II velocities in the SMC fell into two well separated groups. The best cases for SMC interstellar velocities are listed by Feast, Thackeray & Wesselink (1960, Table VIIIb). Although only six objects are involved the division into two velocity groups is rather striking, as may be seen in Fig. 7 when these velocities are plotted. Three Ca II lines give a mean residual velocity of -28 km s^{-1} and the other three of $+7$ km s^{-1}. As shown in Fig. 7 the agreement with the planetaries (means of -32 and $+9$ km s^{-1}) is excellent.

Downloaded from https://academic.oup.com/mnras/article/140/3/345/2602684 by guest on 20 August 2022

© Royal Astronomical Society • Provided by the NASA Astrophysics Data System

1968MNRAS.140..345F

The recent, more detailed 21 cm work (Hindman & Balnaves 1967; Hindman 1967) shows that the H I velocity pattern is quite complex. These results are partially illustrated by Fig. 8, which is an adaptation of Fig. 18(i) of Hindman (1967). This shows the residual 21 cm peak velocities in a strip $\pm 0°{\cdot}5$ on either side of a line in position angle 55° through the point 1^h03^m, $-72°\,45'$ which is taken as 0°. Whether or not this is the major axis of the SMC is irrelevant to the present purpose. The existence of two (or more) peaks in many directions is evident in this figure as is also the great complexity shown by the high resolution

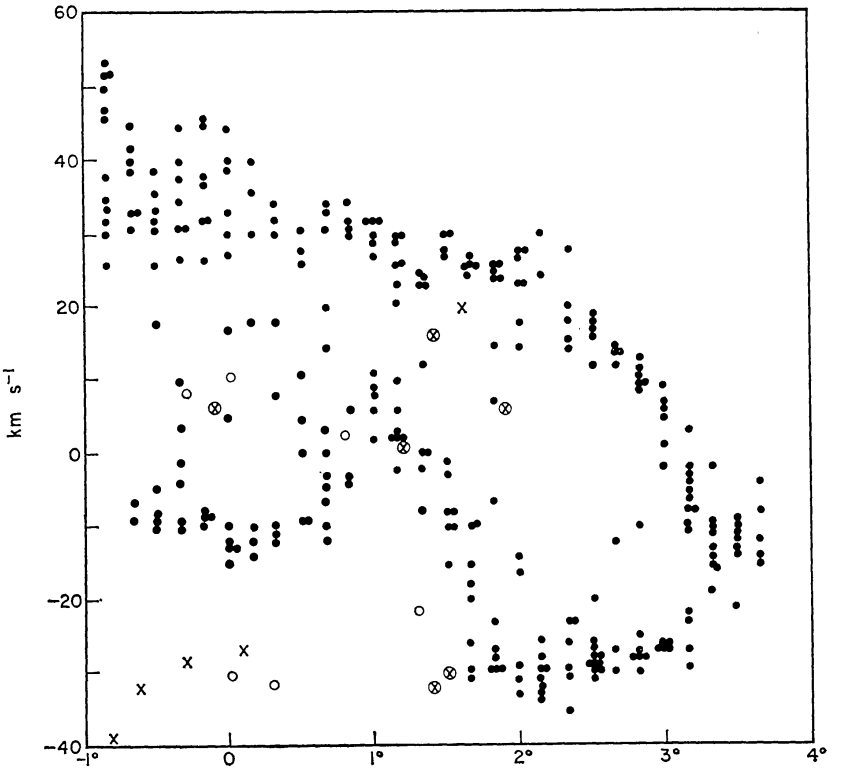

FIG. 8. *The velocity pattern in the SMC along Hindman's major axis. Ordinate: velocity corrected for solar motion and galactic rotation. Abscissa: angular distance along axis (preceding to the right). Filled circles are 21 cm peaks from Hindman* (1967, *Fig.* 18(*i*)). *Crosses are planetary nebulae, those circled being within* 1° *of Hindman's axis. Open circles are Ca II interstellar velocities.*

work. The figure also indicates two points which are discussed in considerable detail by Hindman; the large and practically continuous range of velocity peaks present in the central core of the SMC (at slightly over +1° in the present plot) and the tendency of the peak velocities to define two rings in the diagram on either side of the core. The planetary nebulae are also shown plotted in Fig. 8. They come from a wider region of the SMC than the 21 cm points; the ones within $\pm 1°$ of the axis are indicated by circled crosses. Seven of the eleven planetaries seem to be associated in a general way with the ring-like features. Four of the planetaries with negative velocities (about -30 km s^{-1}) and lying between $-1°$ and $+0°{\cdot}3$ in the plot, fall conspicuously off the general distribution of H I points.

Downloaded from https://academic.oup.com/mnras/article/140/3/345/2602684 by guest on 20 August 2022

© Royal Astronomical Society • Provided by the NASA Astrophysics Data System

1968MNRAS.140..345F

However, these four planetaries all lie a considerable distance from Hindman's axis so that agreement with the particular distribution of H I points shown in Fig. 8 would not necessarily be expected. Furthermore, the 21 cm results shown in Fig. 8 do at least indicate a considerable mass of gas moving at about -30 km s^{-1} over a fairly wide area of the SMC. There was little evidence of this in the earlier survey (Fig. 7). The six interstellar Ca II lines discussed above are also repeated in Fig. 8. From the present point of view the most interesting feature of the Ca II velocities is the fact that two of them project near the four ' divergent ' planetaries at about 0° and -30 km s^{-1}. Hindman (1964) in fact deduced that there were H I peaks corresponding to these two Ca II velocities (at residual velocities of -20 and -23? km s^{-1}). These 21 cm peaks are not evident in the contours plotted by Hindman & Balnaves (1967). More detail is apparently present in the SMC than is seen in these plots. It seems reasonable in the light of the above discussion to take the view that so far as the large scale pattern of motions in the SMC is concerned the motions of the planetaries bear some considerable similarity to that of the interstellar gas. This is especially true in respect of the double peaked velocity profiles which indicate the probable existence of two or more distinct gas–star complexes moving with different velocities in the same line of sight. It is therefore concluded that, as in the LMC, the overall motions of gas and planetaries is basically similar though detailed agreement is poor because of age differences.

The interpretation of the double peaks in the 21 cm profiles has constituted an important problem for some while. The latest of several solutions that have been proposed is that of Hindman (1967) who considers the existence of two or perhaps three large expanding shells of gas. Because of the considerable expansion velocities involved these structures must be quite young ($\sim 10^7$ years). Since it has been seen that in the SMC as elsewhere the planetaries are old objects it would seem impossible to fit them into the expanding shell picture despite the general similarities of their motions to that of the gas. The present evidence certainly suggests that multiple peaked frequency distributions are characteristic of objects of a wide range of ages in the SMC and any explanation applicable only to the youngest subsystem would seem to be unsatisfactory.

It has been suggested (Hindman 1967; *cf.* also Basinki, Bok & Bok 1967) that in the ' core ' region of the SMC we are viewing a barred system practically end on. Non-circular motions in such a system with gas and stars flowing out of both ends of the bar might well explain the observed velocity pattern especially as the two major expanding shells of Hindman are symmetrically placed with respect to this ' core ' (Hindman 1967, Fig. 11). Indeed the sides of these two shells towards the core region seem hardly distinguishable from the general structure of the core in the velocity–intensity–position plots of Hindman & Balnaves (1967). A detailed study of all the available data with this hypothesis in mind would appear to be desirable.

6. *The excitation classes of the Magellanic Cloud planetaries.* Investigations of galactic planetaries have shown that the relative intensities of the various emission lines change markedly from one object to another (*cf.* Aller 1956). This is chiefly the result of differing excitation temperatures. An examination of the present spectra of Magellanic Cloud planetaries shows that a similar range of excitation is present. It is relatively simple to recognize 10 classes defined chiefly by the following inequalities:

Downloaded from https://academic.oup.com/mnras/article/140/3/345/2602684 by guest on 20 August 2022

© Royal Astronomical Society • Provided by the NASA Astrophysics Data System

1968MNRAS.140..345F

	Class		
	0	$H\beta \gg N_2$	4471 He I > 4686 He II
Low	1	$H\beta > N_2$	
	2	$H\beta \approx N_2$	
	3	$H\beta < N_2$, $H\epsilon > 3967$[Ne III]	
	4	$H\beta \ll N_2$, $H\epsilon \ll 3967$[Ne III]	
Medium	5	$H\beta \gg 4686$ He II	
	6	$H\beta > 4686$ He II	
	7	$H\beta$ very slightly stronger than 4686 He II	4471 He I < 4686 He II
High	8	$H\beta \approx 4686$ He II	
	9	$H\beta < 4686$ He II	

The ratios, though easy to recognize apply of course only to the present telescope and spectrograph combination and baked Kodak IIaO plates (in a very few early cases Kodak 103aO plates). Class O does not apply to any of the present Cloud planetaries. It is the class into which diffuse nebulae, both in the Galaxy and in the Magellanic Clouds, commonly fall. Only one of the objects in Table I falls into this class; SMC N68 which is now known to be a small diffuse nebula (*cf.* Section 5). The LMC object N44A is discussed in the remarks to Table I, it is classified as a high excitation diffuse nebula. It is the highest excitation diffuse nebula yet found in the Magellanic Clouds, yet it is of low excitation compared with the majority of planetaries. On these grounds alone therefore, it is reasonable to conclude that the majority of objects in the present survey must be planetary nebulae.

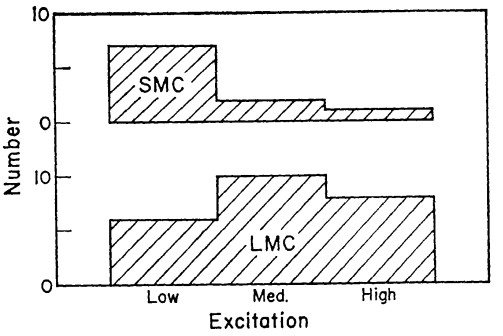

FIG. 9. *Frequency distribution of excitation classes for planetary nebulae in the Magellanic Clouds.*

Because of the relatively small number of objects involved in the present survey it is best to discuss excitation in terms of the three broad groups shown above; low, medium and high excitation. Fig. 9 shows the frequency distribution of the excitation classes in the two clouds. Even considering the small number of objects involved, there appears to be a definite indication of a difference in frequency distribution between the two clouds. Low excitation planetaries are found to predominate in the SMC. A quantitative comparison with the Galaxy in this respect would be very desirable but this is not at present possible. However even a rough comparison with the excitation classes (on a somewhat different system) assigned by Page (1942) to galactic planetaries, suggests that these are much more like the LMC than the SMC in the frequency distribution of excitation classes.

Downloaded from https://academic.oup.com/mnras/article/140/3/345/2602684 by guest on 20 August 2022

© Royal Astronomical Society • Provided by the NASA Astrophysics Data System

1968MNRAS.140..345F

Page's galactic results show an increasing frequency of planetaries with increasing excitation class. The interpretation of these results is not entirely straightforward since the frequency distributions may be affected by selection effects (e.g. selection according to magnitude). Some evidence for effects of this kind is shown in Fig. 10 where the frequency distributions of excitation classes are shown separately for LMC planetaries brighter and fainter than $B^N = 17{\cdot}0$. There is an indication of an increasing frequency of high excitation planetaries with decreasing luminosity. It is evidently desirable to follow up these tentative indications in much greater detail. It is hoped to discuss the chemical composition of the Magellanic Cloud planetaries at a later date.

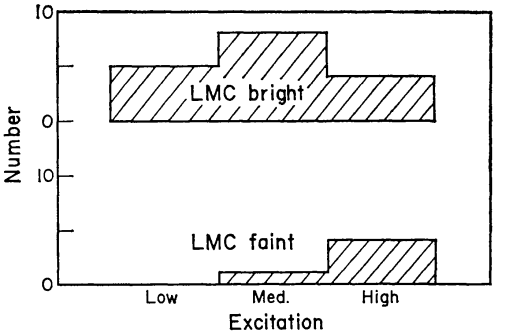

FIG. 10. *Frequency distribution of excitation classes for bright and faint planetary nebulae in the LMC. The division into two groups was made at* $B^N = 17^m{\cdot}0$.

Acknowledgments. I should like to express my thanks to Mrs J. A. Clayton for her extensive help with the numerical work and to my wife for drawing the figures. Dr A. D. Thackeray very kindly read a first draft of the paper and suggested various improvements.

Radcliffe Observatory,
Pretoria,
South Africa.
1968 *February.*

References

Aller, L. H., 1956. *Gaseous Nebulae*, Chapman and Hall, London.
Basinski, J. M., Bok, B. J. & Bok, P. F., 1967. *Mon. Not. R. astr. Soc.*, **137**, 55.
Bok, B. J., Gollnow, H., Hindman, J. V. & Mowat, M., 1964. *Aust. J. Phys.*, **17**, 404.
Bolton, J. G., 1965. *Symposium on the Magellanic Clouds*, p. 33, Canberra.
Bowen, I. S., 1955. *Astrophys. J.*, **121**, 306.
Feast, M. W., Thackeray, A. D. & Wesselink, A. J., 1960. *Mon. Not. R. astr. Soc.*, **121**, 337.
Feast, M. W., Thackeray, A. D. & Wesselink, A. J., 1961. *Mon. Not. R. astr. Soc.*, **122**, 433.
Feast, M. W. & Thackeray, A. D., 1963. *Mem. R. astr. Soc.*, **68**, 173.
Feast, M. W., 1961. *Mon. Not. R. astr. Soc.*, **122**, 1.
Feast, M. W., 1964a. *Mon. Not. R. astr. Soc.*, **127**, 195.
Feast, M. W., 1964b. *Observatory*, **84**, 266.
Feast, M. W., 1966. *Mon. Not. R. astr. Soc.*, **132**, 495.
Feast, M. W., 1967. *The Galactic dynamics and Galactic Distribution of the Planetary Nebulae*, IAU Symposium No. 34, in press.
Harrison, G. R., 1939. *M.I.T. Wavelength Tables*, John Wiley, New York.
Henize, K. G., 1956. *Astrophys. J., Suppl. Ser.*, **2**, 315.
Henize, K. G. & Westerlund, B. E., 1963. *Astrophys. J.*, **137**, 747.
Hindman, J. V., 1964. *Nature, Lond.*, **202**, 377.

Downloaded from https://academic.oup.com/mnras/article/140/3/345/2602684 by guest on 20 August 2022

© Royal Astronomical Society • Provided by the NASA Astrophysics Data System

1968MNRAS.140..345F

Hindman, J. V., 1967. *Aust. J. Phys.*, **20,** 147.
Hindman, J. V. & Balnaves, K. M., 1967. *Aust. J. Phys., Astrophys. Suppl.*, No. 4.
Hindman, J. V., Kerr, F. J. & McGee, R. X., 1963. *Aust. J. Phys.*, **16,** 570.
Johnson, H. M., 1959. *Publs astr. Soc. Pacif.*, **71,** 301.
Lindsay, E. M., 1961. *Astrophys. J.*, **66,** 169.
Lindsay, E. M. & Mullan, D. J., 1963. *Ir. Astr. J.*, **6,** 5 (Armagh Contributions No. 41).
McGee, R. X., 1964. *Aust. J. Phys.*, **17,** 515.
McGee, R. X. & Milton, J. A., 1966a. *Aust. J. Phys.*, **19,** 343.
McGee, R. X. & Milton, J. A., 1966b. *Aust. J. Phys., Astrophys. Suppl.*, No. 2.
Moore-Sitterly, C. E., 1945. *A Multiplet Table of Astrophysical Interest*, Princeton Contributions No. 20.
Page, T. L., 1942. *Astrophys. J.*, **96,** 78.
Trumpler, R. J. & Weaver, H. F., 1953. *Statistical Astronomy*, p. 126, University of California Press.
de Vaucouleurs, G., 1960. *Astrophys. J.*, **131,** 265.
de Vaucouleurs, G., 1964. *The Galaxy and the Magellanic Clouds*, p. 269, Australian Academy of Science, Canberra.
Webster, B. L., 1965. *Symposium on the Magellanic Clouds*, p. 29, Canberra.
Wesselink, A. J., 1966. *Astrophys. J.*, **71,** 185.
Westerlund, B. E. & Smith, L. F., 1964. *Mon. Not. R. astr. Soc.*, **127,** 449.
Westerlund, B. E. & Rodgers, A. W., 1959. *Observatory*, **79,** 132.
Westerlund, B. E., 1967. *Planetary Nebulae in the Magellanic Clouds*, IAU Symposium No. 34, in press.

Downloaded from https://academic.oup.com/mnras/article/140/3/345/2602684 by guest on 20 August 2022

© Royal Astronomical Society • Provided by the NASA Astrophysics Data System